Supplementary Material to the article
"Magnetic topological alloys based on the Cd_3As_2 Dirac semimetal: The doping by Cr, Mn, and Fe atoms"

1. Electronic density of states (DOS) within a wide energy range

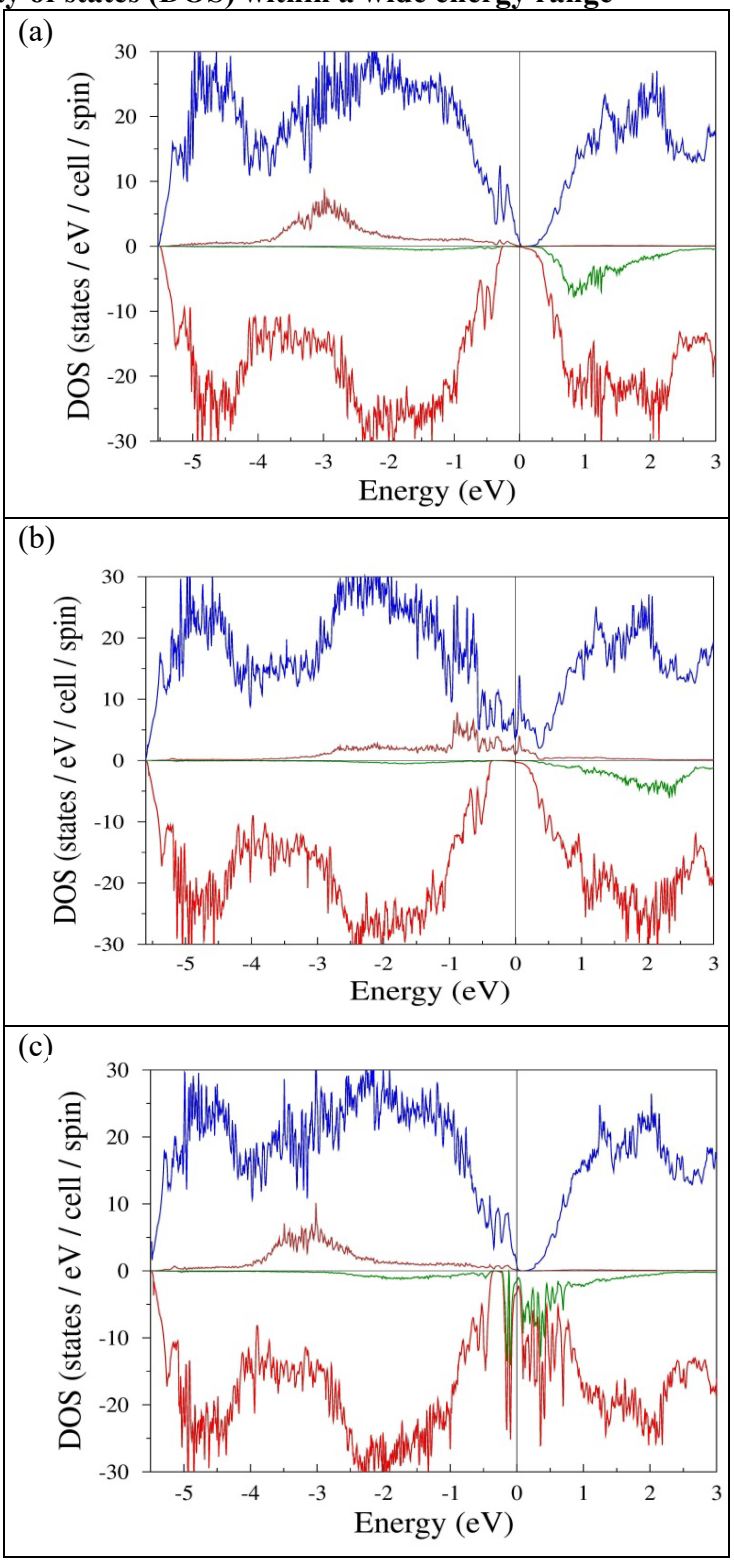

Fig. S1. Electronic density of states (DOS) $N_s(E)$ within a wide energy range for (a) $(Cd_{1-x}Mn_x)_3As_2$, (b) $(Cd_{1-x}Cr_x)_3As_2$ and (c) $(Cd_{1-x}Fe_x)_3As_2$ alloys with the ferromagnetic (FM) spin ordering. The $N_\uparrow(E)$ и $N_\downarrow(E)$ are shown in red and blue, respectively, whereas the partial contributions of the dopant states $N_{M\uparrow}(E)$ and $N_{M\downarrow}(E)$ – in brown and green.

In Cd_3As_2 Dirac semimetal, the apex of the Dirac cone lies exactly at the Fermi level (E_F). In $(Cd_{1-x}M_x)_3As_2$ alloys (M = Mn, Cr, and Fe), this feature usually disappears due to two mechanisms: (1) the non-isoelectronic nature of doping, and (2) the hybridization of the Weyl (Dirac) cone states with the M 3*d*↑ and M 3*d*↓ orbitals of dopants. The latter mechanism is particularly important because it provides different energy shifts for the spin-up and spin-down cone states. The centers of the impurity M 3*d*↑ and M 3*d*↓ bands can be located outside the energy range around the Fermi level, being sometimes shifted by several eV away from it. To give a clearer picture of the energy distribution for M 3*d*↑ and M 3*d*↓ states, we show in Fig. S1 the total and partial (corresponding to the contribution of M atoms) electronic densities of states $N_s(E)$ and $N_{M,s}(E)$, $s = \uparrow, \downarrow$ in the energy range from –5.5 eV to +3.0 eV relative to E_F. As we can see in Fig. S1, all three alloys exhibit the 3*d*↑–3*d*↓ band splitting by 3–4 eV, which provides the existence of an energy window without any M 3*d* states for one of spin directions near E_F. The Weyl (Dirac) cones remain untouched just within such windows.

2. Effect of the spin-orbit coupling (SOC) on the band structure

$(Cd_{0.96}Mn_{0.04})_3As_2$

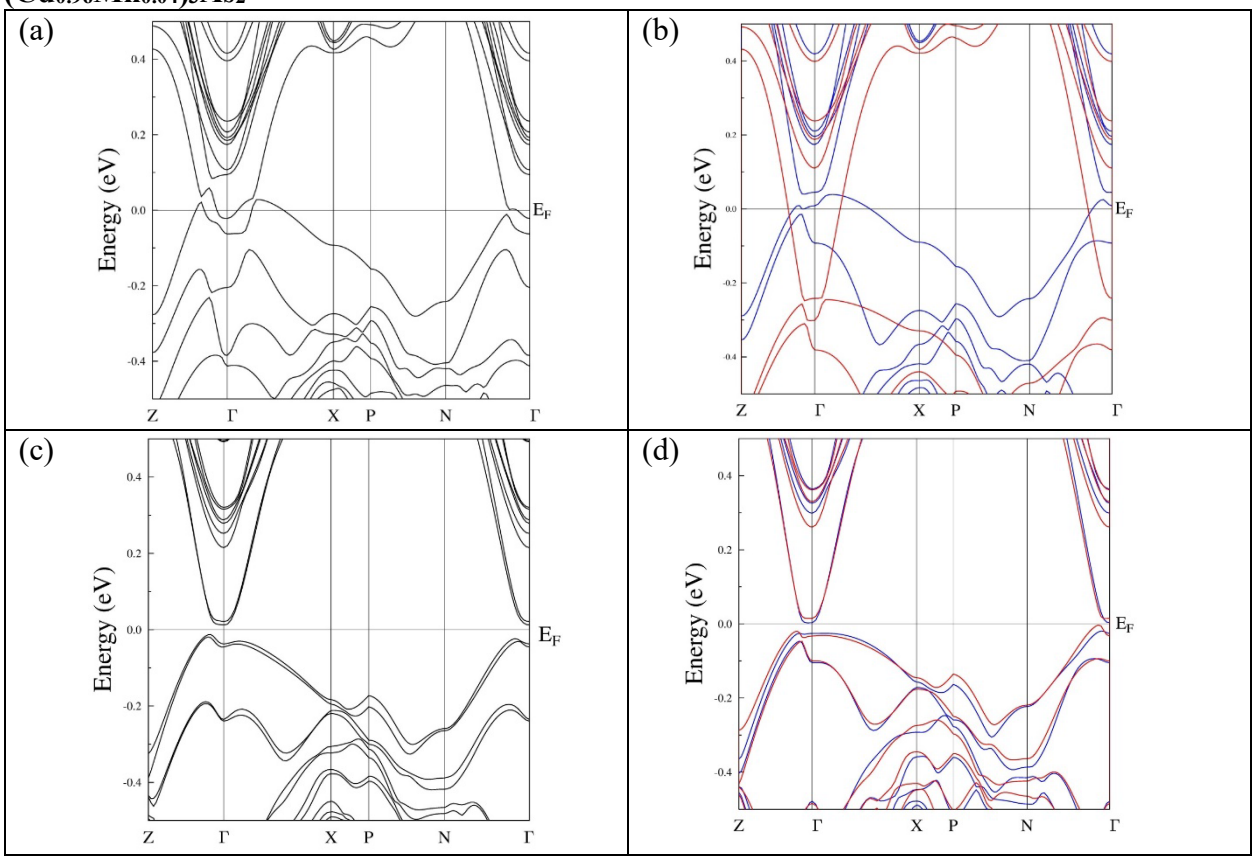

Fig. S2. Comparison of the band structure of $(Cd_{0.96}Mn_{0.04})_3As_2$ calculated taking (panels (a) and (c)) and not taking (panels (b) and (d)) into account the spin-orbit coupling. Panels (a) and (b) correspond to the ferromagnetic (FM) spin ordering of two impurities in the supercell shown in Fig. 1a of the main text, whereas panels (c) and (d) correspond to the antiferromagnetic (AFM) spin ordering. Blue and red colors in panels (c) and (d) denote spin up and spin down states, respectively. In the AFM case, a slight difference between blue and red curves is due to an nonequivalence of the crystallographic positions of impurities.

$(Cd_{0.96}Cr_{0.04})_3As_2$

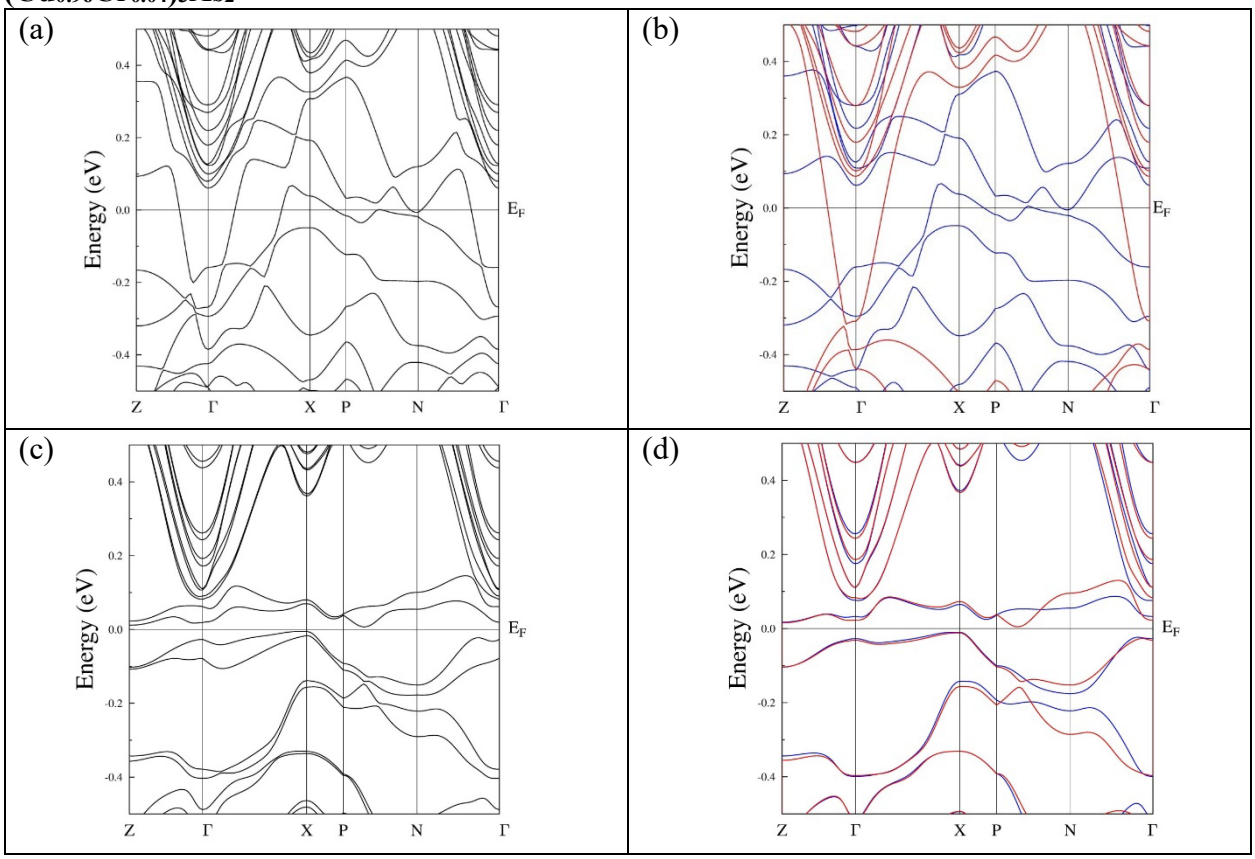

Fig. S3. Band structure of $(Cd_{0.96}Cr_{0.04})_3As_2$. Notation is the same as in Fig. S2.

$(Cd_{0.96}Fe_{0.04})_3As_2$

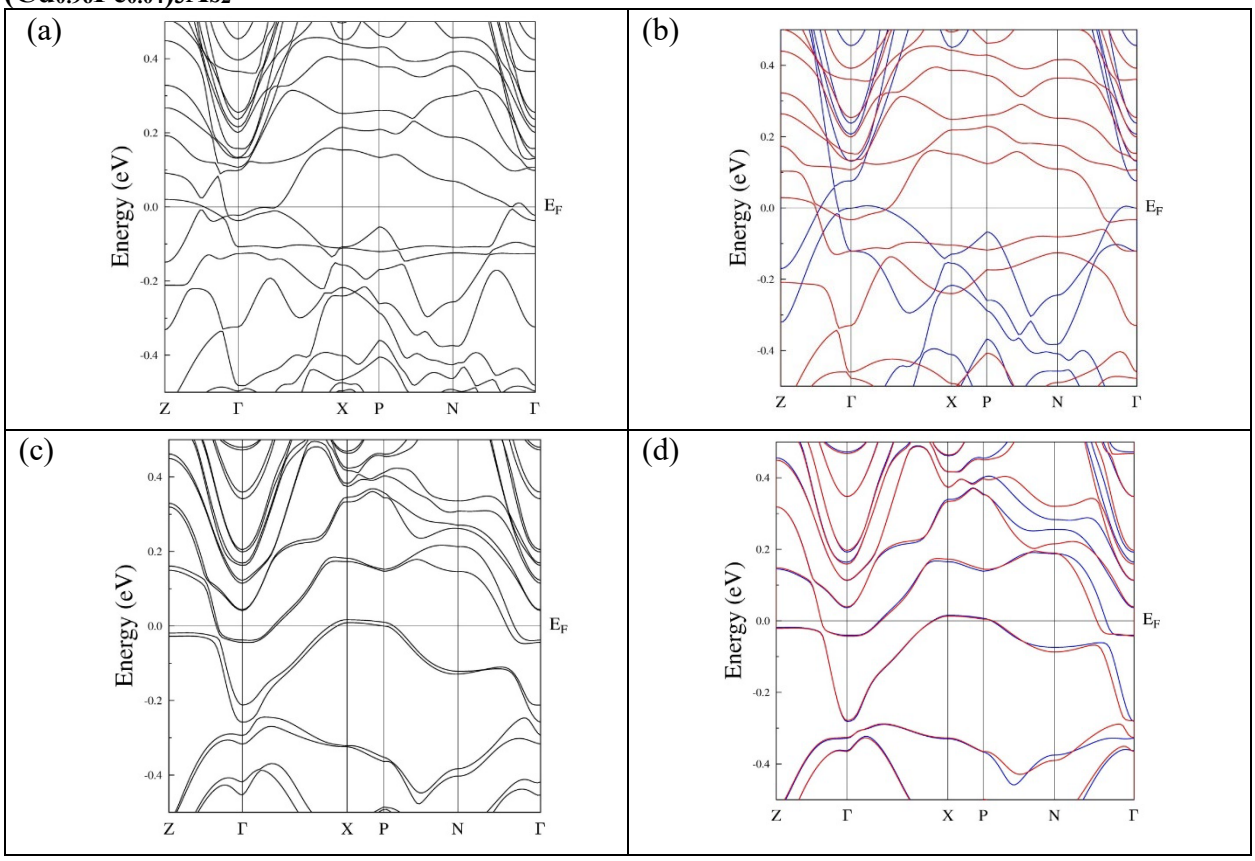

Fig. S4. Band structure of $(Cd_{0.96}Fe_{0.04})_3As_2$. Notation is the same as in Fig. S2.

The band structure of FM $(Cd_{1-x}M_x)_3As_2$ alloys calculated taking SOC into looks complicated because of the spin-up and spin-down band mixture (Figs. S2a-S4a). At the first glance, the identification of the Weyl cone (WC) among such a spaghetti-like SOC band is quite difficult. To solve this problem and estimate the effect of exchange splitting on the band structure of FM $(Cd_{1-x}M_x)_3As_2$, we turned off SOC (Figs. S2b–S4b). After neglecting SOC, the band structure becomes decomposed into spin-up and spin-down bands that makes WC↑ and WC↓ clearly visible in Figs. S2b–S4b. A careful comparison shows that bands calculated with and without SOC are rather similar. The main difference occurs near the crossing points between spin-up and spin-down bands where these bands are hybridized and mixed by SOC. The range near the crossing points, where the band mixing occurs, is not large because of the relatively small strength of SOC. This turning-off technique also reveals the effect of exchange splitting on WC, which can destroy or keep untouched WC depending on the $3d\uparrow$- and $3d\downarrow$-band energies related to M atoms. In view of its advantages, this technique is used in the band structure analysis throughout the paper.